EIC Compton Polarimetry and Simulations June 2018 Report for eRD15

Alexandre Camsonne[1], Dipankgar Dutta[4], Michael Sullivan[5], David Gaskell[1], Cynthia Keppel[1], Fanglei Lin[1], Juliette Mammei[2], Joshua Hoskins[2], Michael J. Murray[3], Christophe Royon[3], Nicola Minafra[3], Vasiliy Morozov[1], Haipeng Wang[1], and Robert Rimmer[1]

[1] Thomas Jefferson National Accelerator Facility
[2] University of Manitoba
[3] Kansas University
[4] Mississipi State University
[5] SLAC National Accelerator Laboratory

June 27^{th} 2018

1 Introduction

As discussed at the in the midterm report, the focus of our final analysis was refining our software tools, expanding and widening our systematics analysis to the full energy range expected for EIC running, and assessing the impact of halo on the asymmetry measurement. Building on the simulations and analysis development framework developed thus far we present a full analysis rates, backgrounds, and asymmetries for three separate energies. This analysis includes a full model of the Compton chicane, developed in GEMC. Results from the our model were cross-checked with our GEANT3 model when appropriate, though the geometric models differ slightly. We also present an analysis of the halo contribution to the detector rate due to scattering from the apertures found upstream (downstream) of the Compton interaction point.

2 Progress Report Section

2.1 Past

2.1.1 What was planned for this period?

Here is the list of task that were approved by the committee for fiscal year 2017.

- more realistic design of Roman Pot geometry in simulation (was simply a plate for now)
- optimize number of strips and strip size for best systematics with as few channels as possible
- optimization of thin window for improved systematics
- determination of expected accuracy of the measurement
- determine the contribution of beam induced background using molflow and synrad package

2.1.2 What was achieved ?

- more realistic design of Roman Pot geometry in simulation (was simply a plate for now) : detector encased in a box to evaluate rescattering from the bottom of the box. We are in discussion with the TOTEM collaboration to have access to geometries and technical drawing of an existing Roman Pot.

- optimize number of strips and strip size for best systematics with as few channels as possible : at 3 GeV (worst case scenario) dividing the number of strips by 5 does not affect the result, so 40 strips could be sufficient instead of the initial 200. This makes it easier to manage on the electronics side. Nevertheless the strip size might be still limited by the rate by strip.
- optimization of thin window for improved systematics : the 500 μm thick window was shown to have minimal impact on the polarization extraction at high energy. A correction might be needed at 3 GeV but the accuracy of 1% level seems achievable at all energies. The design might need to be improved (one plane in vacuum) if accuracies better than 0.5 % are needed.
- determination of expected accuracy of the measurement : all polarization extracted were within 1% of the generated polarization, so the Roman Pot Design can reach 1% polarization accuracy at all energies.
- determine the contribution of beam induced background using molflow and synrad package : eRD21 implemented the synchrotron radiation process in GEMC and have expertise from eRD21 to use Molflow. A low statistics Synchrotron power deposit was done using GEMC. A more advanced design of the beamline is needed to evaluate the pumping speed. We are also working with Michael Sullivan to use his code to generate the synchrotron photons more efficiently for this study.

2.2 Future plan

We will not ask for additional funds for next cycle. Plan is to have an agreement with TOTEM to import Roman Pot geometry in the simulation and have a first draft design of the chamber and pumping element to evaluate background coming from beam induced outgassing. More study of systematics from different parameters such as field or position accuracies will be done. A final report summarizing all the work for the project will also be written.

3 Synchrotron radiation study

Since the synchrotron radiation process is now available in GEMC 2.6, we can turn the process on. A stainless plate was put before the detector to evaluate the power deposit in the vacuum chamber as shown in Fig. 1.

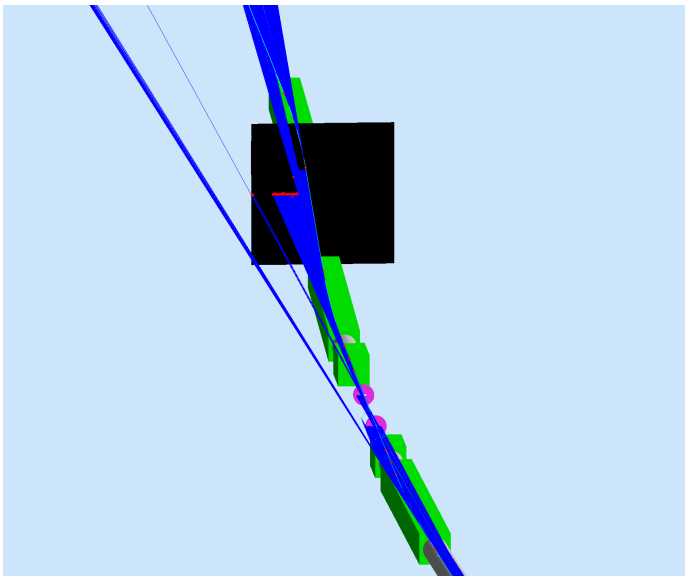

Figure 1: 5 GeV electron beam transported through the chicane. A plane was placed before the Compton Electron Detector to determine the synchrotron radiation power deposit

A preliminary power density of about 3 W per mm^2 was found for 3A of 5 GeV beam (Fig. 3). This feature in GEMC will be useful to study synchrotron background in the detector though rate

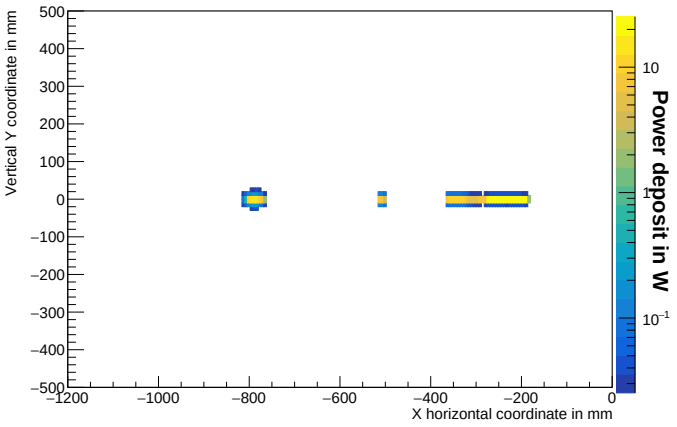

Figure 2: Synchrotron power XY distribution

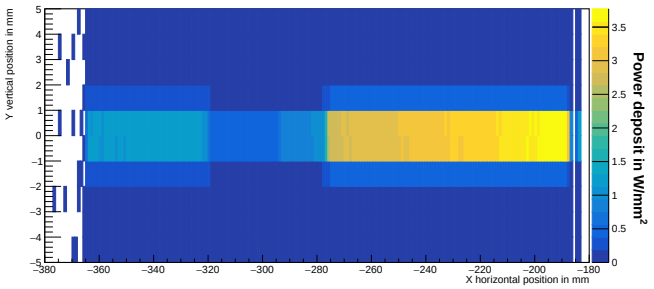

Figure 3: Synchrotron power XY distribution with 1mm x 1mm bins, giving power in W per mm^2

of event generation is about 1 KHz. For power evaluation for outgassing we plan to use EGCS or SynRad on simplified geometry. A cross check of GEMC will be done with the other packages to make sure the low energy setting of GEANT4/GEMC are correctly set to study synchrotron radiation.

Beam induced outgassing will be evaluated in the next cycle after a preliminary setup of vacuum pumps is done.

4 Software Development

For the purposes of the Compton simulations, a full software suite was developed. We have developed generators that provided both Compton events and an estimate of the halo. With our focus shifting to a wider range of energies and new ambitions of looking at systematics in the electron detector, a more integrated, functional package was needed to avoid constantly reediting ROOT macros. Equally important was the fact that all the software needed to connect straightforwardly to the batch farm at Jefferson Lab. With this in-mind, a fully integrated analysis suite that allowed for easy access scientific computing, fully customizable detector and beam energy parameters, all available to the working group via github, was developed. In addition, the Compton fitting was changed to work with all beam energy settings and allow the detector properties to be changes as need; this is especially important for the detector systematics work.Since out last report most off the development work has slowed in favor of debugging and fine-tuning of the software becoming the core focus. The plan is for the work to continue in the future as needed for planning and studies. For this purpose a full software manual will be included internally at Jefferson lab.

5 Compton Simulation Analysis

5.1 Detector Rate

We have performed GEANT4 simulations to characterize the electron detector rate and signal-to-noise ratio. Simulations were done for a single pass, CW laser with 10 W of power. The beam energies used were 3 GeV, 5 GeV, and 10 GeV at a beam current of 1A. Signal-to-noise results for all energies are shown in figure 4 - 6 respectively. The background rate was simulated by passing beam through the beam pipe with the laser off. The beam pipe was filled with Hydrogen gas at 1 atm to expedite the process and then the rate was scaled to a beam current of 1A and a vacuum of 10^{-9} Torr. In each case the signal is order of magnitude above the background. Contributions from the upstream IP are not included as they were found to be sub-hertz level. Backgrounds due to halo effects are discussed in more detail in Sec. 5.2.

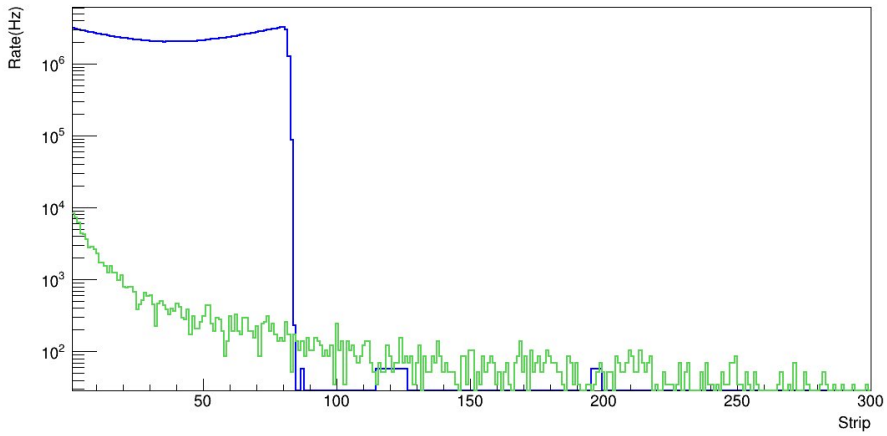

Figure 4: Scattering rate in electron detector at 3 GeV. The Compton scattering rate is shown in blue and the background rate is show in green. The background rate does not include halo or upstream events.

The scattering asymmetry can be formed by simulating the Compton event rate for both helicities and then using the subsequent histograms to build an asymmetry; asymmetries are calculated

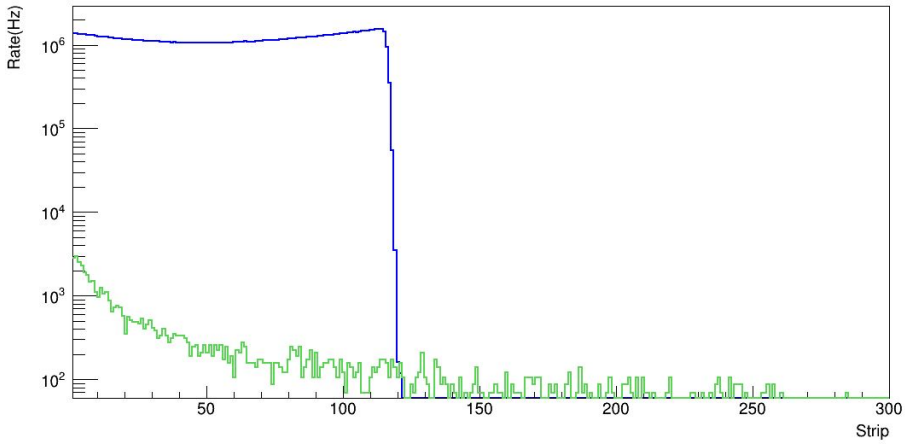

Figure 5: Scattering rate in electron detector at 5 GeV. The Compton scattering rate is shown in blue and the background rate is show in green. The background rate does not include halo or upstream events.

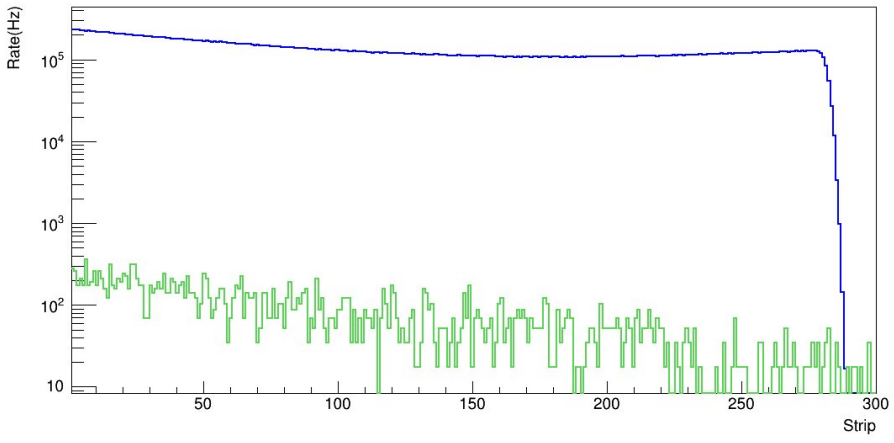

Figure 6: Scattering rate in electron detector at 10 GeV. The Compton scattering rate is shown in blue and the background rate is show in green. The background rate does not include halo or upstream events.

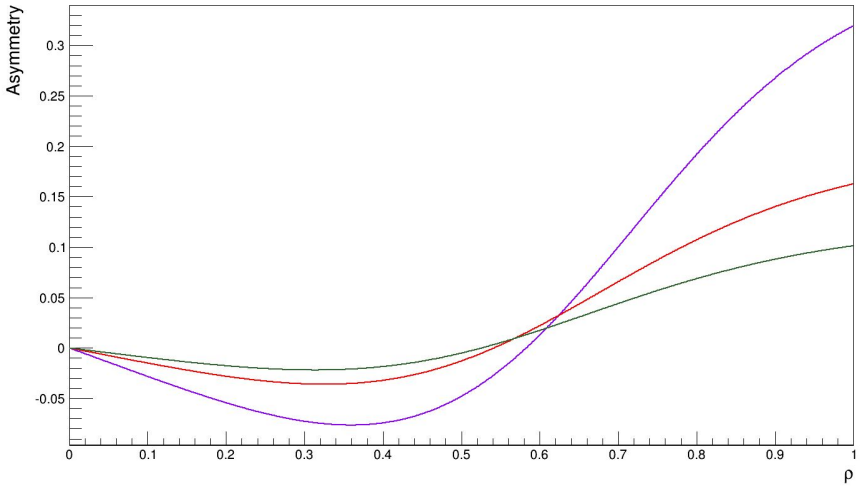

Figure 7: Theoretical asymmetries for each energy level produced by the Compton generator. The asymmetries are 3 GeV (green), 5 GeV (red), 10 GeV (purple) respectively.

on a bin-by-bin basis and the bin error is used for each point. The Compton asymmetry for each energy are plotted versus strip number in figures 8 - 10. For comparison, the expected theoretical asymmetry for all three energies are shown in Fig. 7. The simulated asymmetries match the theoretical expectations.

5.2 Halo Study

Backgrounds due to halo are generated primarily from two sources, halo interaction with apertures associated with a Fabry-Perot cavity in the Compton chicane and direct interaction of the halo at the electron detector. The apertures are an important part of the cavity because they help protect the mirrors from beam excursions but can also generate background in the electron detector. We report results for halo induced backgrounds at energies of 3 GeV, 5 GeV, and 10 GeV below.

The halo was modeled using a double Gaussian distribution as described in the PEPII report and is given by,

$$\frac{dN}{dxdy} = e^{-\frac{x^2}{2\sigma_x^2}-\frac{y^2}{2\sigma_y^2}} + Ae^{-\frac{x^2}{2(S_x\sigma_x)^2}-\frac{y^2}{2(S_y\sigma_y)^2}}.' \tag{1}$$

Results for background rates due to aperture scattering are shown in figures 11 - 13. Background are order of magnitude smaller than the simulated Compton rate. This analysis presents halo rates using an aperture size of $\pm$ 1.5 cm but it should be noted that the rate could be reduced ever further by making the apertures larger; this of course can be done within the bounds of them still serving their purpose of protecting the mirrors.

As the beam propagates along the beam the size of the halo evolves along with the beam profile. There is potential for the halo profile to interact directly with the electron detector if the halo is sufficient large in the detector region. The backgrounds due to direct interaction of the halo with the electron detector are shown in Table 1. The background rate depends on both the amplitude of the halo profile and the halo multipliers, S_x and S_y from Eq. 1 which define the width of the halo. The background rates depend on heavily on the combination of halo multiplier and in the worst case can reach MHz levels.

One key point that must be mentioned is the fact that no good estimate of the halo amplitude, given in Eq. 1 as A, or the halo modifiers, S_x and S_y, exist at the moment. While the rate due to interaction with the apertures is relatively small in comparison to the Compton signal, the rate due to direct interaction with the detector, as seen from the studies in the previous report, is extremely large depending on the choice amplitude. With no estimate on the actual size of the halo however we can only say that the halo has the potential to be significant if not controlled.

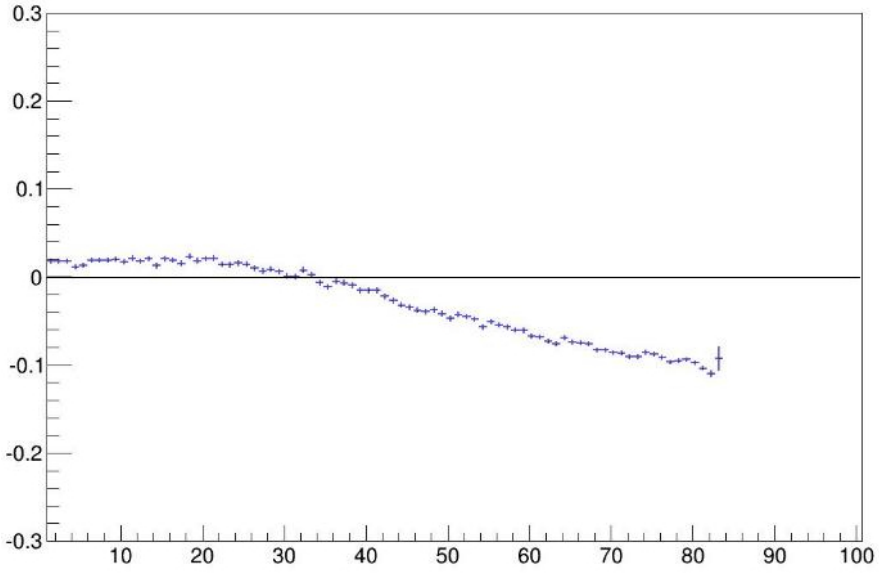

Figure 8: The simulated Compton scattering asymmetry as seen in electron detector at 3 GeV plotted versus strip number.

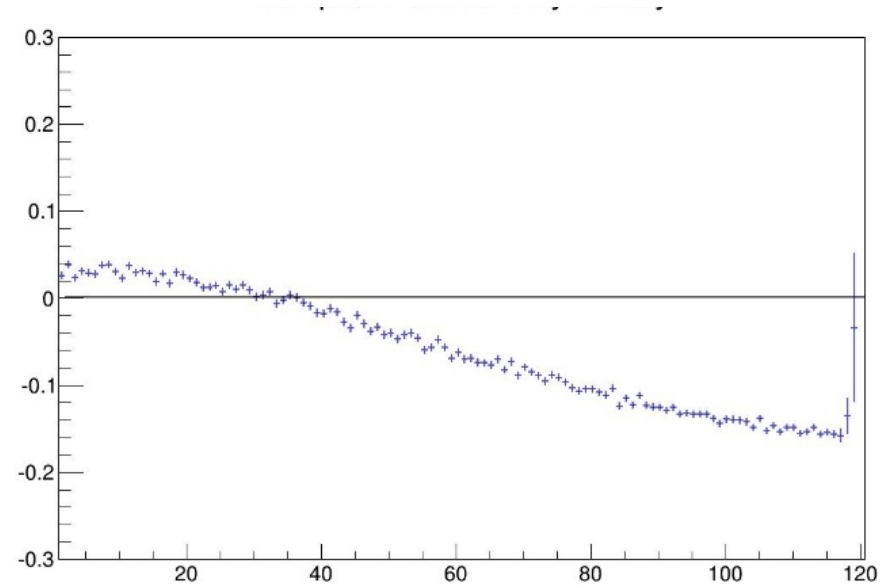

Figure 9: The simulated Compton scattering asymmetry as seen in electron detector at 5 GeV plotted versus strip number.

S_x/S_Y	5	6	7	8	9	10
5	0.0	0.0	0.0	380.2	2708.9	10613.9
6	0.0	0.0	66.5	646.3	2908.5	15920.8
7	0.0	0.0	155.3	620.9	3792.5	14526.7
8	0.0	0.0	88.7	557.6	4505.4	18312.9
9	0.0	0.0	49.9	1368.7	3849.5	20031.7
10	0.0	0.0	0.0	823.7	6273.3	24633.7

Table 1: The halo background rate in kHz due to the halo interacting directly with the electron detector. This table includes data for 5 GeV beam energy.

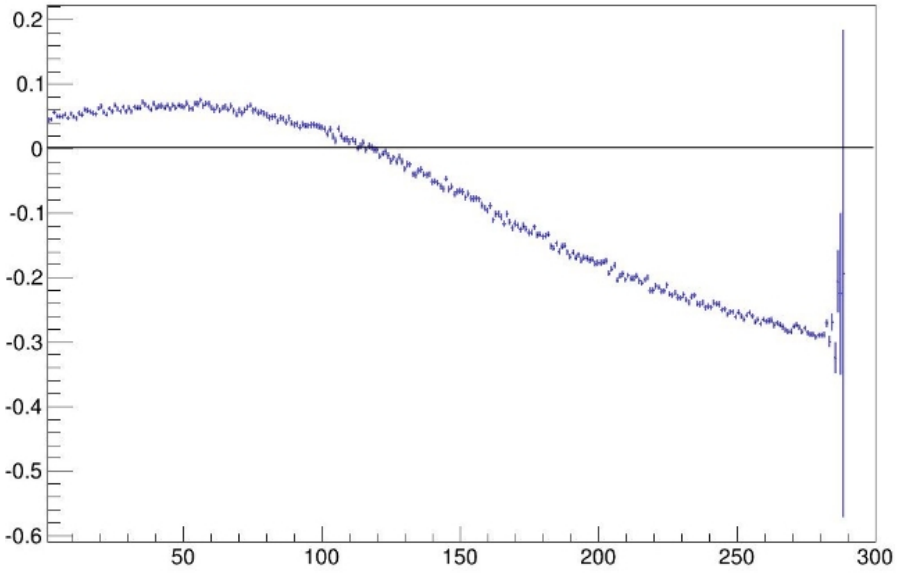

Figure 10: The simulated Compton scattering asymmetry as seen in electron detector at 10 GeV plotted versus strip number.

5.3 Detector Systematics

The goal of the detector study was to determine the expected impact of systematic effects on the polarization extraction. This includes effects due to detector strip width and roman pot window thickness. The polarization extraction is done using fitting software, adapted to the EIC geometry, from the Qweak experiment which uses the geometry of the magnets and the target setup to map the energy as a fraction of the Compton edge to the position on the detector. The asymmetry as a function of strip is then fit and the polarization is extracted. The fits for each energy can be seen in figures 14 - 16

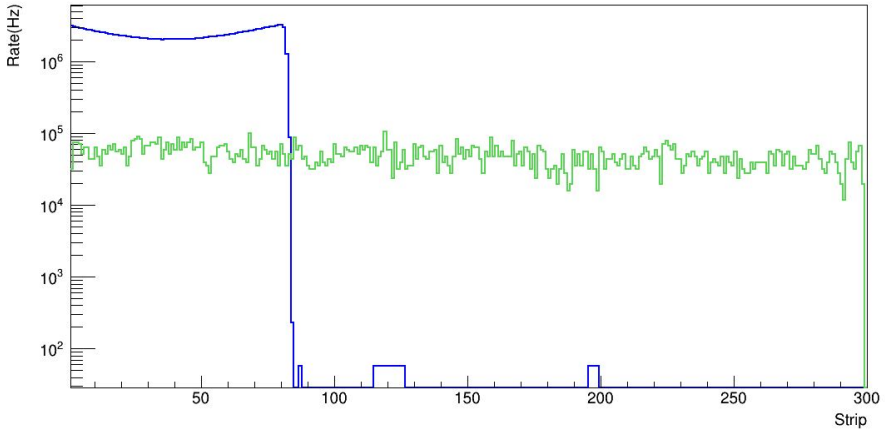

Figure 11: Background due to the halo interacting with the apertures at 3 GeV plotted with the Compton detector rate. This rate can be lowered even further by making the aperture slots slightly bigger.

The strip width study was carried out by simulating the asymmetry in the electron detector and then using the fitting software to calculate the measured polarization. The size of each strip was then varied by changing the binning while keeping the total detector size fixed. Using this we were able to use increasingly fewer strips and look at how the measured asymmetry changed. This gives us the effective minimum resolution of the detector. The results from the study for all energies can be seen in Table 2.

From the fit results the polarization extraction is shown to be moderately insensitive to the

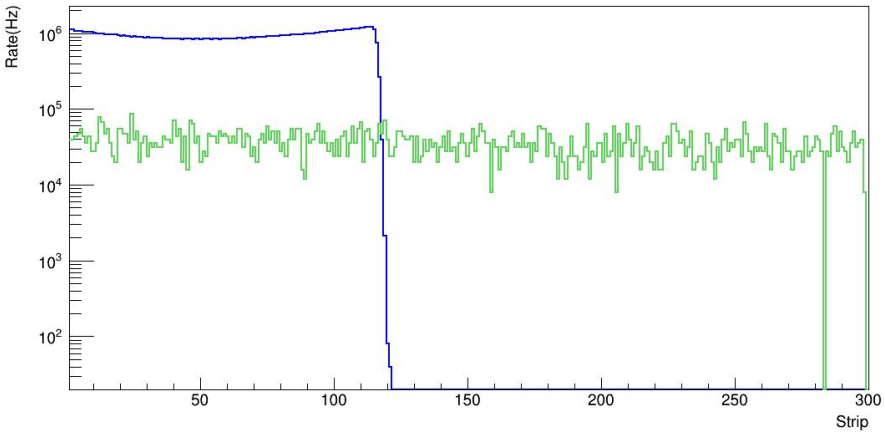

Figure 12: Background due to the halo interacting with the apertures at 5 GeV plotted with the Compton detector rate. This rate can be lowered even further by making the aperture slots slightly bigger.

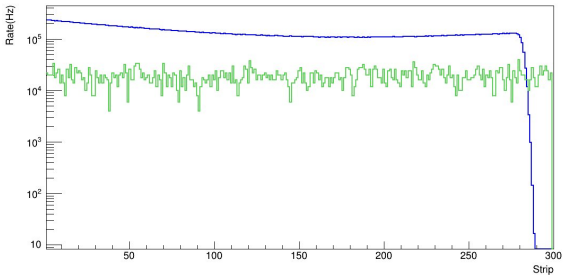

Figure 13: Background due to the halo interacting with the apertures at 10 GeV. This rate can be lowered further by making the aperture slots slightly bigger.

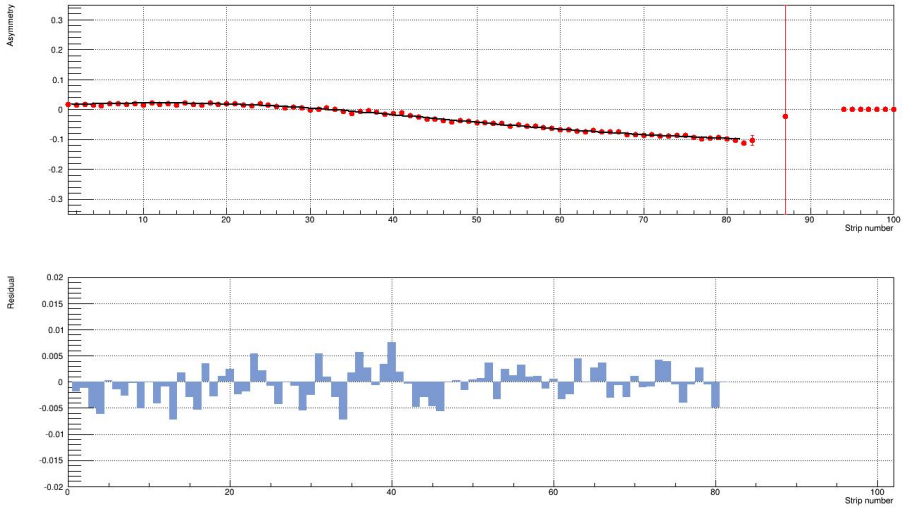

Figure 14: Fit of the Compton asymmetry at 3 GeV. The fit residuals are shown below the fit.

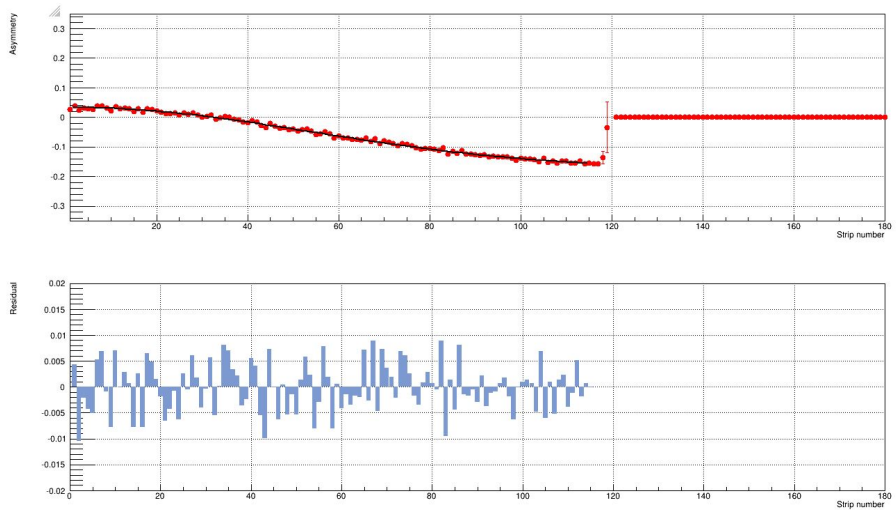

Figure 15: Fit of the Compton asymmetry at 5 GeV. The fit residuals are shown below the fit.

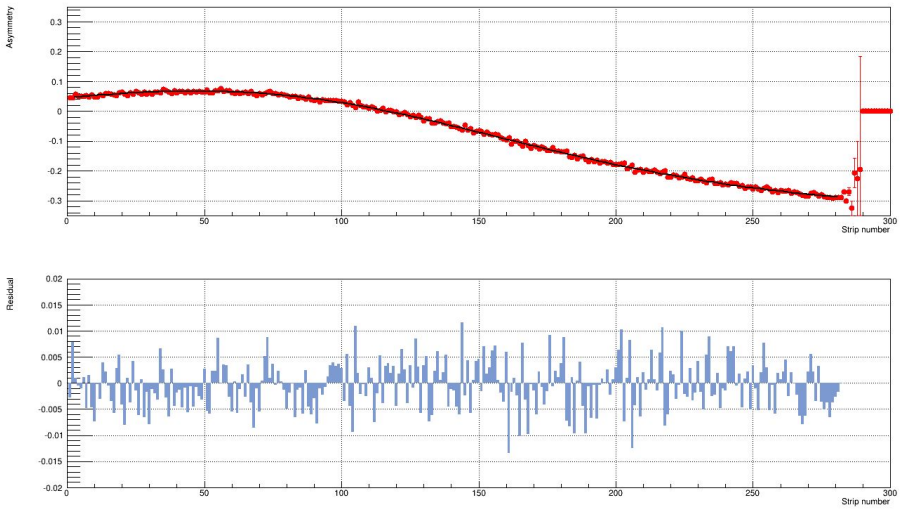

Figure 16: Fit of the Compton asymmetry at 10 GeV. The fit residuals are shown below the fit.

Strip Size	Energy (GeV)	Polarization	χ^2/NDF
240 μm	3	-97.02 ± 0.67	1.02
480 μm	3	-97.97 ± 0.64	1.09
1200 μm	3	-97.43 ± 0.65	2.29
2400 μm	3	-96.01 ± 0.62	4.83
2880 μm	3	-95.25 ± 0.60	6.01
4800 μm	3	-96.20 ± 0.64	7.45
240 μm	5	-97.69 ± 0.58	0.88
480 μm	5	-97.48 ± 0.58	0.83
1200 μm	5	-97.53 ± 0.59	0.97
2400 μm	5	-97.41 ± 0.59	1.02
2880 μm	5	-97.17 ± 0.59	1.23
4800 μm	5	-96.68 ± 0.60	2.29
240 μm	10	-97.19 ± 0.24	1.08
480 μm	10	-97.94 ± 0.23	1.37
1200 μm	10	-97.79 ± 0.23	1.36
2400 μm	10	-97.70 ± 0.23	3.73
2880 μm	10	-97.71 ± 0.26	4.31
4800 μm	10	-97.65 ± 0.23	7.96

Table 2: Polarization extraction results for different strip size. The extraction is moderately insensitive to the strip size and varies with energy slightly.

Energy (GeV)	Window Configuration	Polarization	χ^2/NDF
3	Thin (50μm)	-97.02 ± 0.67	1.02
3	Thick (500μm)	-96.60 ± 0.90	0.95
5	Thin (50μm)	-97.69 ± 0.58	0.89
5	Thick (500μm)	-96.59 ± 0.79	0.99
10	Thin (50μm)	-97.19 ± 0.17	1.17
10	Thick (500μm)	-97.00 ± 0.24	1.17

Table 3: Polarization extraction results for two different window thicknesses. The target chamber was made of stainless steel and fully surrounds the the electron detector.

strip size up to a factor of 10 increase and then only at low energy. As strip size of less than 1200 μm is a safe estimate for all energies. This agrees with previous analysis both from our group and independent estimation made using the GEANT3 model by the polarimetry group at Jefferson lab.

The effects the thickness of target window on the roman pot were also studied by looking at the systematic change in the extracted polarization between a 50 μm window and a 500 μm window. The results are found in 3 and show slight deviation of the central value from the expected polarization of 97% but no change within errors.

6 Summary

There is much that we would still like to accomplish Moving forward. In the last 6 months. We have seen that the signal-to-noise for both beamline and halo background are estimated to be at acceptable levels, with the later estimate being highly sensitive knowledge of the halo properties; with this said, there should be a concerted effort to estimate and control the halo. Moving forward we would like to study more systematic effects on the polarization extraction from sources such as the dipole strength, dipole position, and detector position. There is also interest in looking at the extraction in the remaining three detector planes.